



Evaluation of bacterial adhesion strength on phospholipid copolymer films with antibacterial ability by microfluidic shear devices

Journal:	<i>Journal of Materials Chemistry B</i>
Manuscript ID	TB-ART-03-2021-000657.R1
Article Type:	Paper
Date Submitted by the Author:	02-May-2021
Complete List of Authors:	Kozuka, Yuta; The University of Tokyo, Department of Bioengineering Lu, Zhou; The University of Tokyo, Bioengineering; National Institute for Materials Science, Masuda, Tsukuru; The University of Tokyo, Hara, Shintaro; The University of Tokyo, Bioengineering Kasama, Toshihiro; University of Tokyo; Nagoya University, ImPACT Research Center for Advanced Nanobiodevices Miyake, Ryo; Tokyo Denki Daigaku, ; The university of Tokyo, Graduate school of engineering Isu, Norifumi; LIXIL Corp Takai, Madoka; The University of Tokyo, Bioengineering

ARTICLE

Evaluation of bacterial adhesion strength on phospholipid copolymer films with antibacterial ability by microfluidic shear devices

Received 00th January 20xx,
Accepted 00th January 20xx

DOI: 10.1039/x0xx00000x

Yuta Kozuka^{a†}, Zhou Lu^{a†}, Tsukuru Masuda^a, Shintaro Hara^a, Toshihiro Kasama^a, Ryo Miyake^a, Norifumi Isu^b, and Madoka Takai^{a*}

Biomimetic phospholipid copolymer films are known to possess antifouling properties against protein adsorption and biofilm formation. However, the interactions between bacterial cells and material surfaces are not fully understood. This work investigated the bacterial adhesion strength of phospholipid copolymer films using a shear stress-tunable microfluidic device. The copolymer, comprising 2-methacryloyloxyethyl phosphorylcholine (MPC), 3-methacryloxypropyl trimethoxysilane (MPTMSi), and 3-(methacryloyloxy) propyl-tris(trimethylsilyloxy) silane (MPTSSi), formed crosslinked films on glass substrates; the thickness of the coating film was controlled by the polymer concentration during dip-coating. Polymer films with two typical thicknesses, 20 nm and 40 nm (denoted as C-20 and C-40, respectively), were prepared on the bottom wall of the microfluidic device. After seeding the *S. aureus* in the microfluidic device, several shear stresses were applied to evaluate the adhesion strength of the polymer films. *S. aureus* was found to have weaker adhesion strength on the C-40 surface than on the C-20 surface; numerous bacterial cells detached from the C-40 surface on application of identical shear stress. To mimic the presence of plasma protein, fibrinogen (Fg) was introduced into the device before performing the bacterial adhesion assay. The results showed that the adsorption of Fg promoted *S. aureus* adhesion and strong interactions under shear stress. However, the adhesion strength of *S. aureus* did not affect the Fg adsorption for both the C-20 and C-40 surfaces. Using the shear stress-tunable microfluidic device, we found that the adhesion of *S. aureus* on the thicker and softer phospholipid copolymer was weak, and the cells easily detached under high shear stress.

Introduction

Bacterial adhesion and subsequent biofilm formation leads to serious problems in several areas, including sanitary items,¹ food industry,² marine constructions,³⁻⁴ and medical devices.⁵⁻⁶ To solve these problems, researchers have investigated antibacterial materials, including surface modifications;⁵ these are areas wherein understanding the interaction strength between the material surfaces and the bacterial cells is important. Biofilm formation on materials commences with adsorption of planktonic bacterial cells. The process of establishing irreversible adhesion on a solid surface⁷ through synergistic effects includes van der Waals force, electrostatic attraction, hydrophobic interaction, and protein-modulated molecular and cellular interactions.⁸⁻¹⁰

Typically, prior to the bacterial adhesion, numerous proteins or polysaccharides populate the material surface within seconds or minutes to form a “conditioning film,” which is believed to promote bacterial adhesion.¹¹⁻¹³ For instance, the adsorption of a plasma protein, fibrinogen (Fg),¹⁴⁻¹⁵ provides a specific binding site for the Fg-binding-protein (FgBP) located on the surface of *Staphylococcus aureus*¹⁶⁻¹⁹ and enhances its adhesion strength.²⁰

While designing anti-bacterial materials, preventing protein adsorption on the material surface is a promising strategy.²¹⁻²² In a previous study, we developed a biomimetic phospholipid copolymer coating film comprising 2-methacryloyloxyethyl phosphorylcholine (MPC), 3-methacryloxypropyl trimethoxysilane (MPTMSi), and 3-(methacryloyloxy) propyl-tris(trimethylsilyloxy) silane (MPTSSi) (this copolymer is denoted as PMMMSi subsequently). PMMMSi can significantly reduce the protein adsorption owing to the MPC moiety (Fig. 1).²³ Because the copolymer possesses the silane-coupling MPTMSi moiety, the PMMMSi coating has a crosslinking structure, which contributes to the high stability of the coating and the tunability of thickness and mechanical properties.²⁴ As the concentration of the coating solution increases (~0.2 wt%), the thickness increases and the Young's modulus in water decreases for the obtained film. We further demonstrated that thicker and softer

^a Department of Bioengineering, School of Engineering, The University of Tokyo, 7-3-1, Hongo, Bunkyo-ku, 113-8656, Tokyo, Japan *E-mail: takai@bis.t.u-tokyo.ac.jp

^b LIXIL Corporation, 2-1-1, Ojima, Koto-ku, 136-8535, Tokyo, Japan

† These authors contributed equally to this work.

Electronic Supplementary Information (ESI) available. See DOI: 10.1039/x0xx00000x

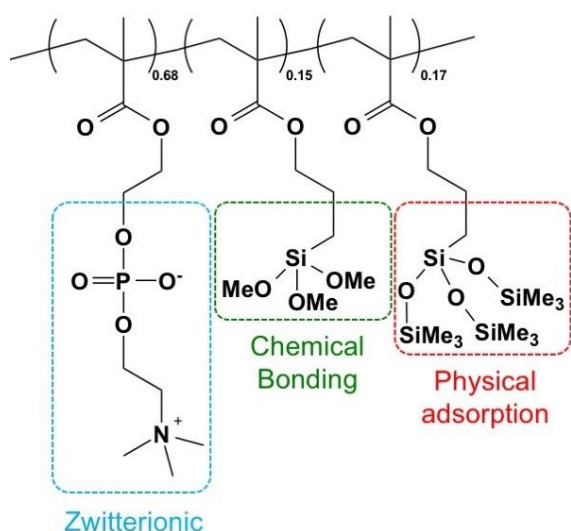


Fig. 1 Chemical structure of poly(MPC-co-MPTMSi-co-MPTSSi) (PMMMSi).

PMMMSi coating films can decrease bacterial adhesion more efficiently.²⁴ This result indicates that the prevention of protein adsorption as well as the mechanical properties of the PMMMSi film play an important role in the anti-adhesiveness of the bacteria. To further understand the interactions between the bacteria and surfaces in terms of their mechanical properties, we focused on the adhesion strength of bacteria on the PMMMSi films.

Researchers have developed various methods to evaluate the interactions between bacteria and material surfaces. For example, atomic force microscopy (AFM)^{20,25–26} is one of the main instruments used to measure the adhesion strength of bacteria to surfaces. AFM can detect bacteria-material interactions in a single cell; however, it is time-consuming and requires intensive operation to obtain sufficient data for statistical analysis. Surface plasmon resonance (SPR)²⁷ and quartz crystal microbalance with dissipation (QCM-D)^{28,29} are also used to measure their interactions. These instruments are superior to others because bacterial adhesion can be analyzed in real time. However, only the mean data of attached bacteria on the sensor surface can be obtained. Thus, a statistical and high-throughput method can provide additional information for bacterial adhesion strength on the surface.

We focused on a hydrodynamic shear assay based on the designed microfluidic device, which allows the investigation of bacterial adhesion strength. The assay was interpreted as the retraction effect of the given shear stress. This strategy imparts benefits such as static and quick response in the bacterial adhesion assays and fast turnaround time for device design and fabrication^{30–34}. The microfluidic device was designed to have suitable dimensions (4.2 mm in width (w), 0.5 mm in height (h), 42 mm in length (L)) that allowed broad observation area for laminar flow at considerably high linear fluid velocities. This phenomenon is important because: 1) the susceptibility of bacterial adhesion was the result of statistical analysis of the substantial data collected from a wide area and 2) bacterial adhesion strength was identified by the endurance test for shear stress.

With the designed microfluidic device, we investigated the adhesion strength of *S. aureus* on bare glass, phospholipid copolymers, PMMMSi, and modified surfaces. The coating films were prepared with thicknesses of approximately 20 and 40 nm in water

(denoted as C-20 and C-40, respectively). A protein (Fg) conditioning film model was formed in the microfluidic device to investigate its influence on bacterial adhesion strength. The adsorption amount of the protein was obtained with quartz crystal microbalance (QCM) measurement, while the bacterial adhesion strength was analyzed by comparing the amounts of bacteria before and after applying the known shear stress. The proposed microfluidic shear device can be used to confirm biofilm susceptibility to materials.

Materials and Methods

Materials

MPC was purchased from NOF Co. (Tokyo, Japan). MPTSSi and MPTMSi were purchased from Shin-Etsu Chemical Co. (Tokyo, Japan). The SylgardTM 184 silicone elastomer kit was purchased from Dow Corning Co. (Michigan, USA). Ammonium chloride, disodium hydrogen phosphate, potassium dihydrogen phosphate, sodium chloride, tryptic soy broth (TSB), 4% paraformaldehyde solution (PFA), methanol, ethanol, acetone, hexane, and 10× Dulbecco's phosphate buffered saline (PBS, without calcium chloride) were purchased from FUJIFILM Wako Pure Chemical Co. (Osaka, Japan). Acetic acid was purchased from Kanto Chemical Co., Inc. (Tokyo, Japan). Loeffler's methylene blue stain solution was purchased from Sigma-Aldrich (Missouri, USA). Glass slides (24 × 60 mm² cover slide) were purchased from Matsunami Glass Ind., Ltd. (Osaka, Japan). Silicon wafers coated with a 10-nm-thick silicon oxide layer (Si/SiO₂ wafer) were purchased from Furuuchi Chemical Co. (Japan).

Preparation and characterization of PMMMSi film

PMMMSi was synthesized by free radical copolymerization of MPC, MPTMSi, and MPTSSi, followed by reprecipitation in acetone/ethanol solvent (20/1, v/v) according to a previous study.²⁴ Methanol solutions containing 0.1 and 0.2 wt% PMMMSi were used for the coating. An aqueous solution containing 1 wt% acetic acid was used as the catalyst and mixed into the polymer solution at an acetic acid aqueous solution/polymer solution of 1/10 (v/v). Si/SiO₂ substrates were sonicated in hexane, ethanol, and acetone for 5 min, followed by cleaning with oxygen plasma (PDC-001, Harrick plasma, USA) at 600 mTorr for 10 min. They were dipped into the coating solution for 30 min and subsequently vacuum dried for 30 min, followed by heating at 70 °C for 3 h.

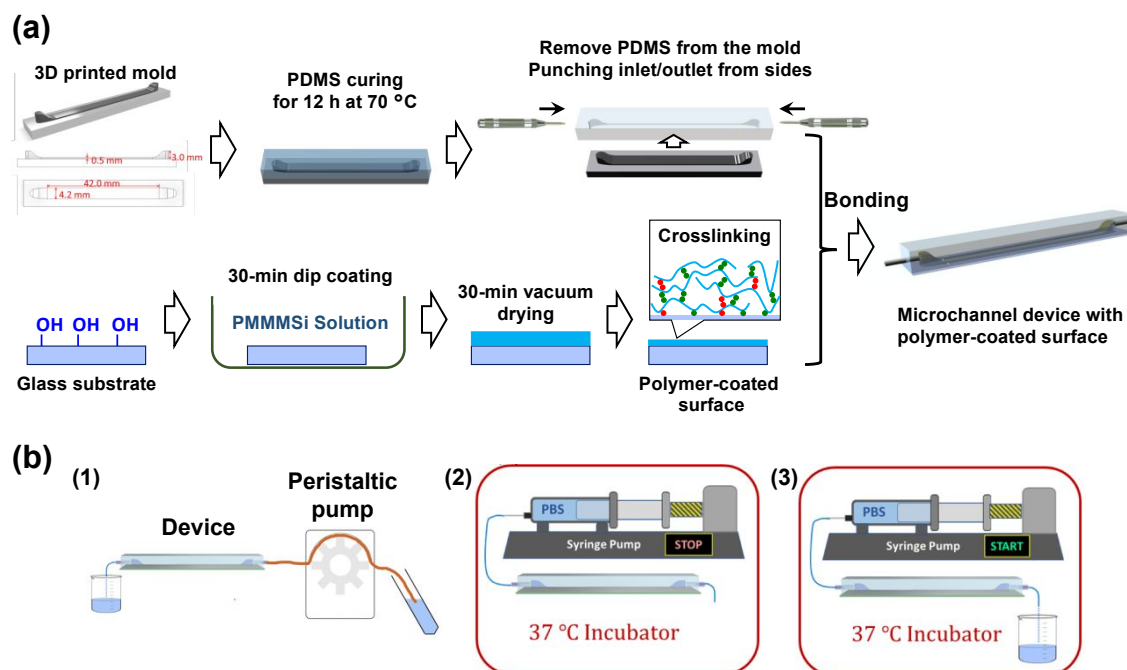


Fig. 2 (a) Preparation of the microfluidic device with polymer-coated bottom surface. (b) Illustration of the process of bacterial adhesion strength assay in the microfluidic device. (1) *S. aureus* suspension was injected into the device using a peristaltic pump with flow rate of 150 $\mu\text{L}/\text{min}$. (2) Bacteria were statically incubated in the microchannel at 37 °C for 2 h. (3) Shear stress was applied by PBS to the microchannel using a syringe pump.

The thickness of the polymer coating films was measured by spectroscopic ellipsometry (M-2000DI, J.A. Woollam Co., Inc. USA) in distilled water. The obtained information was analyzed using the CompleteEASE computer program and fitted according to the effective medium approximation (EMA) model. Surface hydrophilicity was examined by measurements of air bubble contact angles in an aqueous environment (DM-501Hi, Kyowa Interface Science Co., Japan). The substrates modified with polymer films on the top were soaked in water for over 1 h before the measurement to ensure that the hydrophilic phosphoryl choline moiety was exposed to the water phase. An air bubble (10 μL) was placed on the sample surface, and the contact angle was measured. The chemical composition of the polymer coating films was determined using X-ray photoelectron spectroscopy (XPS, JPS-9010MC, JEOL, Tokyo, Japan). The source of the X-ray is aluminum $K\alpha$, and the emission was collected at a take-off angle of 90°. The spectra of C 1s, P 2p, and N 1s states were measured with a step size of 0.1 eV.

Preparation of microfluidic device

The microfluidic devices were prepared using a polydimethylsiloxane (PDMS)-based microchannel. First, a mold for the target microchannel was designed using Autodesk Inventor Professional 2019 computer software and printed using a 3D printer (Objet Eden 260V, Stratasys, Ltd., USA). As shown in Fig. 2 (a), the main fluidic channel is rectangular with a length of 42 mm, width of 4.2 mm, and height of 0.5 mm. Each terminal of the channel is a cylinder with a diameter and height of 3.0 mm. These cylinders serve as the inlet and outlet of the device and connect to the main fluidic channel through smooth slopes. PMMMSi was modified onto glass slides as described above, excluding the heating step. The molded PDMS, which was sonicated in ethanol for 15 min and cleaned with oxygen plasma

treatment, was bonded to the polymer-coated glass slide. The entire device was heated at 70 °C for 3 h to allow the dehydration of the PDMS bonds and silane coupling reaction of the polymer chains. Thus, PMMMSi films were formed at the bottom wall of the channel in the microfluidic device. For the preparation of the non-polymer-coated device as a control, the glass slide was directly bonded onto the molded PDMS after oxygen plasma treatment, followed by the heating step. The fluidic device was constructed by connecting it to a syringe pump system (Legato™ 200, KD Scientific Instrument Services, USA) with a silicon tube (01778, eastsidemed Inc., Japan).

Fg treatment in the microchannel

Fg/PBS (0.1 mg/mL) was pumped through the microfluidic device for 10 min at a flow rate of 100 $\mu\text{L}/\text{min}$, and fresh PBS (Fg free) was pumped through the microfluidic device at the same flow rate for 30 min to remove the non-binding proteins.

Protein adsorption determined by QCM measurement

The QCM sensor, an AT-cut Au-coated quartz crystal with an SiO_2 layer on the top (QSensor QSX 303 SiO_2 , Biolin Scientific, Sweden), was used as the substrate, and the same polymer coating protocol as for the glass slide was followed. After coating, the QCM sensor was moved to a QCM flow module. PBS was pumped over the sensor at a flow rate of 100 $\mu\text{L}/\text{min}$ until the system was balanced. Subsequently, the Fg/PBS (0.1 mg/mL) was pumped through the sensor at the same flow rate for 10 min, and the fluidic medium was changed to fresh PBS (Fg free) and kept running for 30 min to remove the non-binding protein. There were 30 s intervals between the exchanging of the solutions. The resonance frequency shift was

recorded over the third, fifth, and seventh overtones. The weight of the adsorbed Fg was calculated using the following equation:

$$m_{Fg} = -C\Delta f \quad \text{Eq.1}$$

where m_{Fg} is the mass of Fg (ng/cm^2) adsorbed on the QCM sensor, C is the sensor constant ($C = 17.7 \text{ ng}/\text{cm}^2 \text{ Hz}$), and Δf (f in Hz) is the normalized frequency change for each overtone.

Computational fluid dynamics (CFD) characterization

CFD simulation was applied using ANSYS CFX software to analyze the shear stress distribution in the microchannel. The 3D models of the designed device were established in Autodesk Inventor Professional 2019 computer software and meshed into triangular elements. The fluidic liquid near the channel wall was assumed to be non-slip. The simulation was carried out using the Navier-Stokes equations.

Bacterial adhesion strength assay in microfluidic device

S. aureus stocks were frozen at -80°C before experiment. In a biosafety cabinet, the bacteria in a frozen stock were transferred to the 500 μL of TSB medium. After overnight pre-culturing, it was mixed with 25 mL fresh TSB medium and shaken gently at 37°C . The bacteria were proliferated to be an optical density of approximately 0.5 at a light with 600 nm wavelength. The suspension of 20 mL of it was centrifuged at 1500 rpm and medium was removed, followed by adding 20 mL PBS. After centrifuged again, bacteria were suspended to the 10 mL of PBS.

Before using in the experiment, the microfluidic device was infused with PBS for a minimum of 1 h to ensure sufficient exposure of the hydrophilic phosphorylcholine moiety to the aqueous phase.²⁴ bacterial suspension (10^8 cells/mL) in a PBS medium was injected into the microfluidic device using a peristaltic pump at a flow rate of 150 $\mu\text{L}/\text{min}$ (Fig. 2 b-1). Then, the microfluidic device, with bacterial suspension loaded, was carefully connected to a 100-mL syringe that was filled with PBS. The device was sealed and incubated at 37°C for 2 h (Fig. 2 b-2) under static conditions. After opening the outlet of the microfluidic device, 90 mL of PBS was pumped through the device at 15, 30, or 45 mL/min, which corresponded to pressures of 1, 2, and 3 Pa, respectively (Fig. 2 b-3) to generate shear stress over the adhered bacteria at the channel bottom. After applying shear stress, a fixative (2% PFA/PBS) was introduced onto the microfluidic device and maintained at 3°C overnight. Methylene blue was then delivered into the device after fixation, and distilled water was pumped through the microfluidic device to remove any non-bound dye at the end. In the fixation and staining process, the fluid was run at a low flow rate (150 $\mu\text{L}/\text{min}$) to generate negligible shear stress over the adhered bacterial cells on any surface. Thus, only the substantial shear stresses (1, 2, and 3 Pa) are discussed in the following sections.

Data acquisition and image processing

An inverted microscope was used to observe the bacteria adhered to the bottom of the microfluidic device. To quantify the bacterial adhesion on each surface, at least fifteen view fields at $\times 40$ magnification were captured along the centerline of the channel. The images were converted into surface bacterial coverage using the ImageJ software. Surface coverage refers to the area fraction (%) of the adhered bacteria. For each type of sample, the result is the mean

of the calculated view fields. These statistical analyses were performed as Student's t-test.

Results and Discussion

Characterization of PMMMSi films

The weight-average molecular weight of PMMMSi (Fig. 1) was confirmed to be 2.9×10^5 using ^1H -nuclear magnetic resonance (JNM-GX 270, JOEL, Japan), and gel permeation chromatography (JASCO RI-2031Plus detector, Tosoh Co., Japan, column: Agilent PLgel, 5 μm MIXED-C 300 mm, Agilent Co., USA). The PMMMSi films were coated onto Si/SiO₂ substrates to characterize their surface structures and properties. The elemental analysis using XPS revealed that the content of nitrogen and phosphorus from the MPC unit emerged after surface modification (Fig. 3), indicating the successful preparation of the coatings on the substrates. The thicknesses of the PMMMSi films in water were determined using spectroscopic ellipsometry. When the concentrations of the polymer solution in the coating were 0.1 and 0.2 wt%, the thicknesses of the obtained coatings in water were 18.6 ± 2.8 and 41.4 ± 2.0 nm in water, respectively. These polymer coating samples were named C-20 and C-40, respectively, based on their approximate thickness in water. The contact angles of air bubbles in water were $163.2 \pm 3.6^\circ$ and $161.7 \pm 4.4^\circ$, respectively. Detailed characterization results are summarized in Table 1. This result indicates that the obtained surfaces in water are hydrophilic because the MPC moiety is oriented to aqueous media. These characterizations confirmed that the physicochemical properties of the C-20 and C-40 surfaces did not vary significantly.

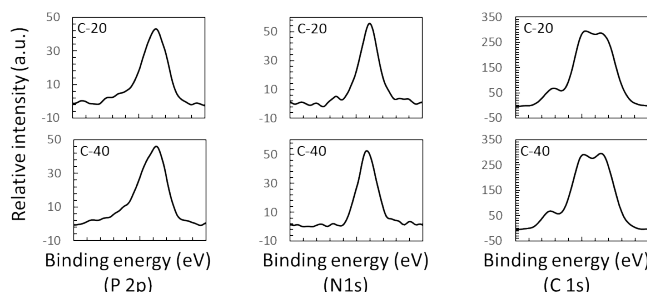


Fig. 3 XPS spectra for P(2p), N(1s), and C(1s) of C-20 and C-40 surfaces.

Table 1. Characteristics of the Phospholipid copolymer films

Surface	Thickness in water (nm) ^a	[P]/[C] ^b	[N]/[C] ^b	Static air contact angle (deg)
C-20	18.6 ± 2.8	0.119	0.107	163.2 ± 3.6
C-40	41.4 ± 2.0	0.124	0.105	161.7 ± 4.4

^a Determined by spectroscopic ellipsometry. The values are expressed as "mean \pm standard deviation".

^b Determined by XPS.

Microfluidic device design

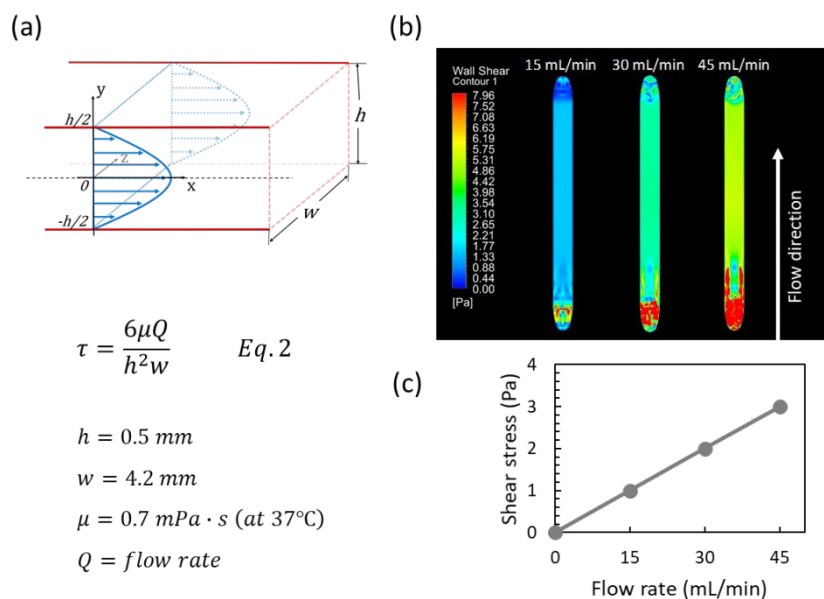


Fig. 4 (a) The velocity distribution and the calculation of the shear stress τ at the bottom wall of the channel, which is a function of the channel height (h), width (w), flow rate (Q), and the viscosity (μ) of the medium; (b) CFD simulation of the shear stress distribution at the bottom of the channel; (c) relationship between the shear stress and the flow rate calculated from Eq 2 (See SI.1).

While designing the microfluidic device, it was assumed that the nm-scale film thickness on the bottom wall would not affect the entire fluidic profile in the microfluidic device. Because the width (w , 4.2 mm) of the rectangular channel used was much larger than its height (h , 0.5 mm) (Fig. 4), the effects of the side walls on the fluidic pattern were negligible; thus, fluidics can be considered to run parallel to the channel. To support this assumption, a CFD simulation was performed. As shown in Fig. 4b, even at a high flow rate (45 mL/min), the shear stress was distributed homogeneously at the bottom wall of the channel. The effect of the side wall was not clear in the results of the CFD simulation, whereas the effects of the inlet and outlet were evident. Nevertheless, the influence from the inlet and the outlet was confined to a limited area, and most of the bottom surface was exposed to uniform shear stress. Based on the parallel plate model and ignoring the effects from the inlet and outlet, the shear stress corresponding to a given flow rate can be calculated using Eq. 2.

$$\tau = \frac{6\mu Q}{h^2 w} \quad \text{Eq.2}$$

Note that the water molecules at the proximity of the channel walls were not considered to move along the main fluent body (non-slip condition). In these ways, by setting the height of the channel at 0.5 mm, the applied shear stress was controlled up to 3 Pa with keeping the laminar flow condition at the flow rate of 45 mL/min.

Study of bacterial adhesion strength with shear stress

The microfluidic device provided precise control of shear stress to assess the bacterial adhesion strength. We focused on three typical values of shear stress generated on the microchannel bottom wall: 1, 2, and 3 Pa. These shear stresses are similar in a human artery.³⁵ A "0 mPa" value was set to obtain the standard information of bacterial initial attachment in which the PBS flow was skipped and the PFA fixation and methylene blue staining occurred immediately after the 2 h static incubation period. Each bottom surface of the channel was

observed using optical microscopy, and bacterial coverage was calculated (Fig. 5 (a, b)).

In the bacterial adhesion assay of the microfluidic device, we changed the flow rate of the solution to remove weakly attached bacteria while maintaining a constant total volume. On the non-coated glass surface, the coverage of the bacteria was approximately 7%, regardless of the applied shear stress. The bacteria attached to the C-20 and C-40 surfaces behaved differently compared to the non-coated glass. Although bacteria on C-20 remained on the surface when exposed to a shear stress of 1 Pa, it detached after a shear stress of 2 or 3 Pa was applied. For the C-40 surface, the bacterial coverage gradually decreased as the shear stress increased. When the shear stress was increased from 2 to 3 Pa, the bacterial polluted area drastically reduced (from 2.1 to 0.5% in coverage). This decrease can be useful as an indicator of a material's anti-biofouling property in laminar flow.

Bacterial adhesion strength assay in the presence of Fg pre-treatment

Implantable medical devices are usually challenged by fouling of the blood protein, which is found to cover the material surfaces in seconds. Protein adsorption triggers the formation of a "conditioning film." Previous studies have suggested that the existence of the conditioning film promotes the adhesion of bacteria.^{12,36} In this study, a model of Fg-conditioning film was prepared to mimic the real application environment of implanted materials. The microfluidic device was flushed with Fg/PBS solution before bacterial introduction, and then the bacterial adhesion assay was performed in the aforementioned manner.

As shown in Fig. 5 (c, d), the Fg-pretreated non-coated glass surface had 1.6-, 1.7-, and 1.3-fold areas of adhered *S. aureus* than the non-treated surface under 1, 2, and 3 Pa shear stress, respectively ($p < 0.001$). The non-coated glass surface was affected by the Fg pre-treatment and enhanced the *S. aureus* adhesion and

strength. On the other hand, when shear stress was applied over the C-20 or C-40 surfaces, a similar quantity of *S. aureus* was removed from the surface with and without Fg pre-treatment. This result indicated that the C-20 and C-40 surfaces were able to maintain their bacterial anti-adhesiveness even when exposed to Fg.

We hypothesized that the formation of a conditioning film on glass surfaces promoted bacterial adhesion. Thus, we analyzed the Fg adsorption on the SiO₂, C-20, and C-40 surfaces using QCM measurements (Fig. S1 in ESI). The Fg flush over the bare QCM sensor surface (SiO₂ surface) resulted in a rapid drop in the frequency,

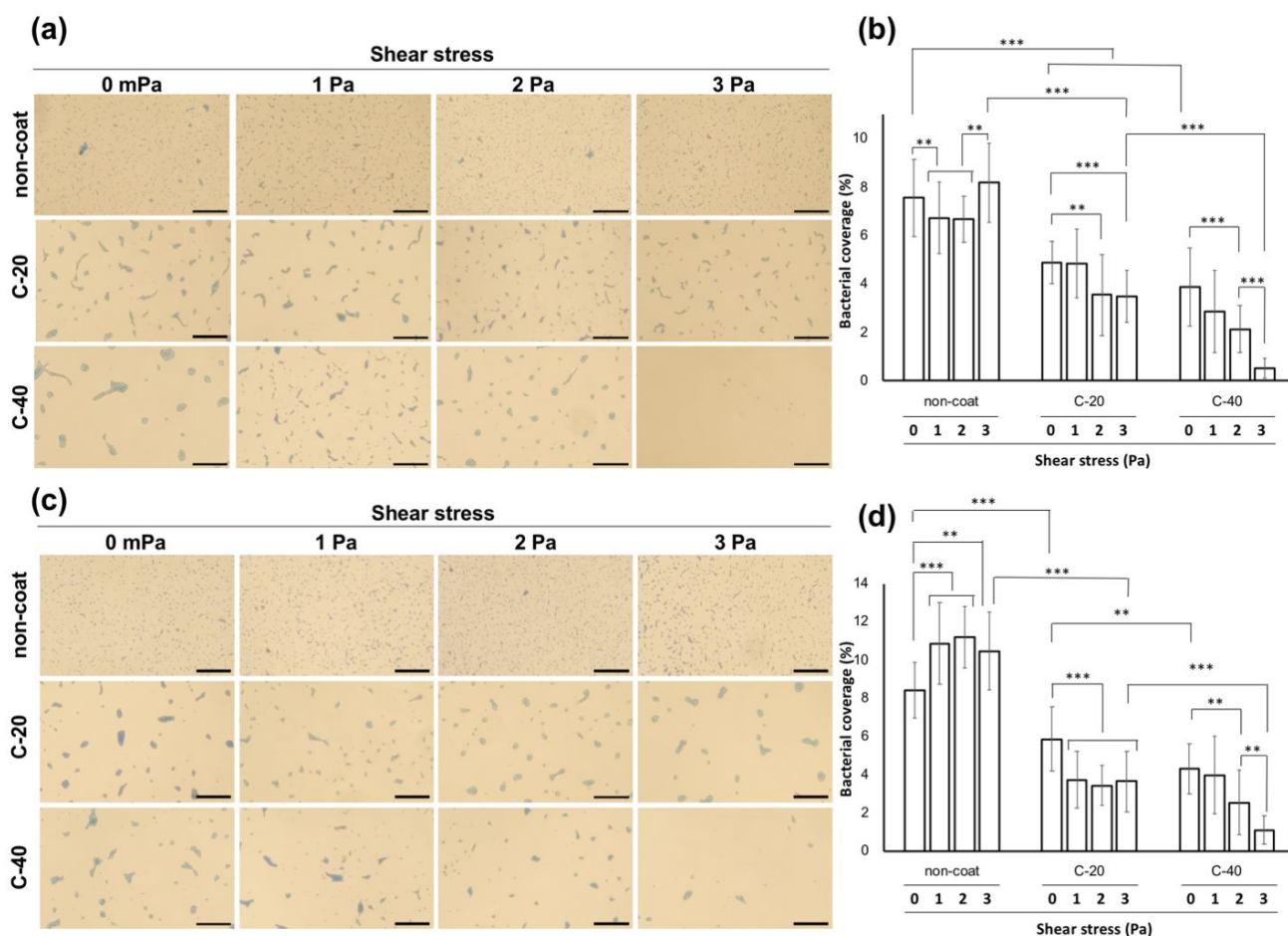


Fig. 5 Bacteria adhered assay; microscopic images of bacteria adhered on the surfaces of non-coated glass, C-20, and C-40 surfaces without PBS exposure (0 mPa) and after the enforcement of 1 Pa, 2 Pa, and 3 Pa shear stress, respectively. (a) without and (c) with Fg application pre-treatment. Scale bars = 50 μm . The results were statistically analyzed to the fraction of adhered bacteria for (b) and (d), which were with and without Fg pre-treatment, respectively. Error bars indicate the standard deviation. ** $p < 0.01$ and *** $p < 0.001$.

indicating that Fg was adsorbed on the surface of SiO₂. After the fluid was shifted to PBS, a slight decrease in the drop frequency was observed owing to the removal of the species adsorbed protein. Finally, the frequency reached a relatively constant level, which represented the quantity of firmly adsorbed protein. The amount of adsorbed protein was estimated to be 960 ng/cm². Meanwhile, no significant Fg adsorption occurred on either C-20 or C-40 (27 and 7.6 ng/cm², respectively). This protein adsorption property is reflected in bacterial adhesion and detachment. The reason that only C-20 and C-40 surfaces could prevent the increase of bacterial pollution by Fg pre-treatment was that the MPC moiety interrupted Fg adsorption and conditioning film formation on them. On comparing Fg adsorption on C-20 and C-40, the amount of adsorbed Fg on C-20 was larger than that on C-40. This trend was the similar to that observed for bacterial adhesion and suggested that bacterial adhesion is related to protein adsorption.

Our experiments revealed that the quantity of bacteria detached from the bottom wall depended on both surface properties and shear stress. C-40 would be softer than C-20 because of the thicker film of C-40.²⁴ Here, the density of the coating films of C-20, and C-40 is the almost same as approximately 1.0 g/cm³,²³ and the Young's moduli of C-20 and C-40 were estimated to be 107 ± 21 MPa and 14 ± 2 MPa, respectively,²⁴ in our previous study. Thus, as thickness and softness increased, the bacterial detachability was enhanced. These results indicate that the strength of the bacteria-surface interaction depends on the mechanical properties of the surfaces used. Thus, microfluidic devices capable of controlling the shear stress on biomimetic phospholipid polymer films facilitated an understanding of bacteria-material interactions. Such devices can contribute to future research on the interactions between bacteria and surfaces.

Conclusions

A shear stress-tunable and polymer-coated microfluidic device for the investigation of bacterial adhesion strength was developed using a 3D printed mold. The CFD simulation indicated that the shear stress in the channel was controlled by the flow rate. The bacterial adhesion strength among phospholipid copolymer coating films with different thicknesses was evaluated by changing the flow rate. Note that bacteria on the C-40 surface was dramatically removed as the shear stress was increased. The phospholipid copolymer coating films reduced the adhesion strength of the *S. aureus*; thicker and softer film exhibited enhanced bacterial anti-adhesiveness. When the surface was exposed to a fibrinogen as a conditioning-film-formation protein, the phospholipid copolymer films maintained their antifouling properties, while the control glass surface did not.

The microfluidic device provides an easy and reliable method for the estimation of bacterial adhesion susceptibility for a variety of surfaces under multiple conditions; thus, the proposed device can serve as a useful tool in the investigation of bacterial adhesion behaviors and antibacterial surface development.

Conflicts of interest

There are no conflicts to declare.

Acknowledgements

This research was partially supported by the Medical Research and Development Programs Focused on Technology Transfers: Development of Advanced Measurement and Analysis Systems (AMED-SENTAN). Zhou Lu would like to thank the Ministry of Education, Culture, Sports, Science and Technology-Japan (MEXT) and the China Scholarship Council (CSC) for their support in his doctoral program.

References

- S. Özcan, N. Çalış Açıkbaz and G. Açıkbaz, *Anadolu Univ. J. of Sci. Technol. A Appl. Sci. and Eng.* 2017, **18**, 1, 122–130.
- Y. Liu, Y. Jiang, J. Zhu, J. Huang and H. Zhang, *Carbohydr. Polym.* 2019, **206**, 412–419.
- S. Chen, P. Wang and D. Zhang, *Corrosion Sci.* 2014, **87**, 407–415.
- P. Wang, Z. Lu and D. Zhang, *Corrosion Sci.* 2015, **93**, 159–166.
- C. Adlhart, J. Verran, N. F. Azevedo, H. Olmez, M. M. Keinänen-Toivola, I. Gouveia, L. F. Melo and F. Crijns, *J Hosp Infect* 2018, 1–11.
- D. Lebeaux, J. M. Ghigo and C. Beloin, *Microbiol. Mol. Biol. Rev.* 2014, **78**, 3, 510–543.
- N. Siboni, M. Lidor, E. Kramarsky-Winter and A. Kushmaro, *FEMS Microbiol Lett* 2007, **274**, 1, 24–29.
- K. Hori and S. Matsumoto, *Biochemical Engineering Journal* 2010, **48**, 3, 424–434.
- R. M. Donlan, *Emerging Infectious Diseases* 2002, **8**, 9, 881–890.
- M. Hermansson, *Colloids. Surf. B Biointerfaces* 1999, **14**, 1, 105–119.
- R. Murga, J. M. Miller, R. M. Donlan, *J Clin Microbiol* 2001, **39**, 6, 2294–7.
- A. J. Slate, D. Wickens, J. Wilson-Nieuwenhuis, N. Dempsey-Hibbert, G. West, P. Kelly, J. Verran, C. E. Banks and K. A. Whitehead, *Colloids Surf B Biointerfaces* 2019, **173**, 303–311.
- G. S. Lorite, C. M. Rodrigues, A. A. de Souza, C. Kranz, B. Mizaikoff and M. A. Cotta, *J Colloid Interface Sci* 2011, **359**, 1, 289–95.
- C. F. Wertz and M. M. Santore, *Langmuir* 2002, **18**, 706–715.
- T. A. Horbett, *J Biomed Mater Res A* 2018, **106**, 10, 2777–2788.
- A. L. Olsson, P. K. Sharma, H. C. Mei and H. J. Busscher, *Appl Environ Microbiol* 2012, **78**, 1, 99–102.
- D. N. Eidhin, S. Perkins, P. Francois, P. Vaudaux, M. Höök and T. J. Foster, *Mol Microbiol* 1998, **30**, 2, 245–257.
- Y. A. Que, J. A. Haefliger, L. Piroth, P. Francois, E. Widmer, J. M. Entenza, B. Sinha, M. Herrmann, P. Francioli, P. Vaudaux and P. Moreillon, *J Exp Med* 2005, **201**, 10, 1627–35.
- M. K. Boden and J. I. Flock, *Infect. Immun.* 1989, **57**, 8, 2358–2363.
- P. Herman-Bausier, C. Labate, A. M. Towell, S. Derclaye, J. A. Geoghegan and Y. F. Dufrêne, *PNAS* 2018, **115**, 21, 5564–5569.
- G. Xu, P. Liu, D. Pranantyo, L. Xu, K.-G. Neoh and E.-T. Kang, *Ind. Eng. Chem. Res.* 2017, **56**, 49, 14479–14488.
- S. E. Kim, C. Zhang, A. A. Advincula, E. Baer and J. K. Pokorski, *ACS Appl. Mater. Interfaces* 2016, **8**, 14, 8928–8938.
- K. Nagahashi, Y. Teramura and M. Takai, *Colloids. Surf. B Biointerfaces* 2015, **134**, 384–391.
- Z. Lu, E. A. Q. Mondarte, K. Suthiwanich, T. Hayashi, T. Masuda, N. Isu and M. Takai, *ACS Appl. Bio Mater.* 2020, **3**, 2, 1079–1087.
- H. H. Fang, K. Y. Chan and L. C. Xu, *J. Microbiol. Methods*, 2000, **40**, 89–97.
- F. Alam and K. Balani, *J. Mech. Behav. Biomed. Mater*, 2017, **65**, 872–880.
- P. Subramanian, F. Barka-Bouaifel, J. Bouckaert, N. Yamakawa, R. Boukherroub and S. Szunerits, *ACS Appl. Mater. Interfaces*, 2014, **6**, 5422–5431.
- T. Leino, M. Raulio, M. Salkinoja-Salonen, P. Stenius and J. Laine, *Colloids. Surf. B Biointerfaces*, 2011, **86**, 1, 131–139.
- K. Otto and M. Hermansson, *J. Bacteriol.*, 2004, **186**, 226–234.
- H. Sun, C. W. Chan, Y. Wang, X. Yao, X. Mu, X. Lu, J. Zhou, Z. Cai and K. Ren, *Lab chip* 2019, **19**, 17, 2915–2924.
- S. Siddiqui, A. Chandrasekaran, N. Lin, N. Tufenkji and C. Moraes, *Langmuir* 2019, **35**, 26, 8840–8849.
- W. B. Lee, C. C. Chien, H. L. You, F. C. Kuo, M. S. Lee and G. B. Lee, *Lab chip* 2019, **19**, 2699–2708.
- M. P. Zarabadi, F. Paquet-Mercier, S. J. Charette and J. Greener, *Langmuir* 2017, **33**, 8, 2041–2049.
- H. Lu, L. Y. Koo, W. M. Wang, D. A. Lauffenburger, L. G. Griffith and K. F. Jensen, *Anal. Chem.* 2004, **76**, 5257–5264.

ARTICLE

Journal Name

- 35 S.K. Samijo, J.M. Willigers, R. Barkhuysen, P.J.E.H.M. Kitslaar, R.S. Reneman, P.J. Brands, A.P.G. Hoeks, *Cardiovasc. Res.*, 1998, 39, 515-522.
- 36 V. Jokinen, E. Kankuri, S. Hoshian, S. Franssila and R. H. A. Ras, *Adv. Mater.* 2018, **30**, 24, 1705104.